Structural phase transition in CaH_2 at high pressures

J. S. Tse,[1] D. D. Klug,[2] S. Desgreniers,[3] J. S. Smith,[3] R. Flacau,[3] Z. Liu,[4] J. Hu,[4] N. Chen,[5] and D. T. Jiang[6]
[1]*Department of Physics and Engineering Physics, University of Saskatchewan, Saskatoon, Saskatchewan, Canada S7N 5E2*
[2]*Steacie Institute for Molecular Sciences, National Research Council of Canada, Ottawa, Ontario, Canada K1A 0R6*
[3]*Laboratoire de physique des solides denses, Department of Physics, University of Ottawa, Ottawa, Ontario, Canada K1N 6N5*
[4]*Geophysical Laboratory, Carnegie Institution of Washington, 5251 Broad Branch Road Northwest, Washington, DC 20015, USA*
[5]*Canadian Light Source, University of Saskatchewan, Saskatoon, Saskatchewan, Canada S7N 0X4*
[6]*Department of Physics, University of Guelph, Guelph, Ontario, Canada N1G 2W1*
(Received 12 October 2006; revised manuscript received 16 February 2007; published 26 April 2007)

The structural and vibrational properties of CaH_2 have been examined up to 30 GPa at room temperature. Under ambient conditions, CaH_2 has a *Pnma* (cotunnite-type) structure. A structural phase transformation was observed around 15 GPa and completed at 20 GPa. The high pressure structure is identified as hexagonal $P6_3/mmc$. First-principles calculations reproduced the first-order nature of the transition. Since $P6_3/mmc$ is a supergroup of *Pnma* the structural change can be traced back to gradual displacements of the hydrogen atoms from the 4*c* positions in the cotunnite structure to the special 2*a* and 2*d* positions in the hexagonal structure. The observed phase transition pressure is much lower than that predicted for MgH_2.

DOI: 10.1103/PhysRevB.75.134108 PACS number(s): 62.50.+p, 61.10.−i

INTRODUCTION

Alloys of metal hydrides are potential efficient hydrogen storage materials.[1] Simple group I and II hydrides such as LiH and MgH_2, due to low atomic weights of the cations, have been seriously considered as good contenders. On the other hand, hydrides of heavier elements, such as the alkaline metal hydride CaH_2, even with the heavier metal ion, have a favorable H_2 specific mass for safe and efficient generation of hydrogen gas from the reaction with water. Therefore, CaH_2 remains a competitive hydrogen carrier medium.[2] Many properties of metal hydrides have been well characterized. There is substantial interest to explore possible metastable high pressure polymorphs with novel structures and properties that may be quenched to ambient conditions for practical applications.[3,4] Recently, it was predicted that metallic hydrides under high pressure can also be good candidate materials with very high superconducting critical temperatures.[5] These materials are suggested to be potential candidates since it is possible that electronic bands associated with the hydrogen may strongly couple with optical phonons. It was proposed that high-frequency hydrogen vibrations and the low-frequency motions of the metal ions will help to enhance the electron-phonon coupling processes. Metal hydrides are insulators under normal condition. However, like many other materials, it is plausible that they may undergo insulator-metal transitions under pressure. For metal hydrides with heavier and more polarizable ions such as CaH_2 and BaH_2, the metallization transition may even occur at moderate pressures.

Recently, structural transformations have been reported for MgH_2 at high pressure.[6] MgH_2 exists in the rutile structure under ambient pressure.[6] Upon compression, it undergoes successive solid-to-solid transformations. Above 17 GPa it transforms to a cotunnite structure (space group *Pnma*) which is stable up to at least 57 GPa. A high pressure transformation sequence was first suggested from first-principles calculations.[6] Although the exact route found computationally for the structural transition was not identical to that observed, nonetheless the stability of the high pressure cotunnite phase was correctly predicted. Interestingly, another higher pressure phase with the Ni_2In (hexagonal $P6_3$) structure was predicted from the calculations to exist at much higher pressure but has not yet been observed.[4] It should be noted that in the proposed $P6_3$ structure[4] the atoms are located in symmetry sites and the space group is identical to $P6_3/mmc$. In comparison, CaH_2 under ambient conditions already adopts the cotunnite structure.[7,8] The main objective of this study is to investigate the possibility of the existence of a hexagonal phase at moderate pressure.

In this paper, results on x-ray diffraction and Raman spectroscopy and theoretical investigations on the high pressure stability of CaH_2 are reported. A high pressure phase with a hexagonal unit cell was found at pressures higher than 15 GPa. In the next section, the experimental and theoretical procedure will be described. Details of the structure and lattice vibrations and comparison with theoretical calculations will be made in the ensuing paragraphs.

EXPERIMENTAL AND THEORETICAL DETAILS

CaH_2 (99.9%, Sigma Aldrich) was loaded into a diamond anvil cell (DAC) under an Ar inert atmosphere without a pressure medium; since the sample is highly moisture sensitive it hydrolyzes readily with commonly used pressure transmitting media like methanol/ethannol mixture or silicone oil. X-ray diffraction patterns were obtained at beamline X17C at the National Synchrotron Light Source (run 1) and the Hard X-ray Micro-Analysis (HXMA) beamline (run 2) at the Canadian Light Source (CLS). The X17C beamline is equipped with a seven-pole superconducting wiggler with 17.4 cm period operating at 4.2 T. Synchrotron radiation monochromatized to 0.4066 Å with a pair of sagitally bent Si (001) Laue crystals was further focused on the sample with Kirkpatrick-Baez 100 mm × 100 mm mirrors. At the HXMA beamline (run 2), synchrotron radiation from a 63–

pole superconducting wiggler was monochromatized to 0.48595 Å with Si (220) crystals and focused by a Rh coated torodial mirror, further collimated to a spot with a diameter of 30 μm. X-ray diffraction images were recorded on FUJI and ST-VI imaging plates and processed with FIT2D.[9] X-ray diffraction patterns were analyzed using XRDA[10] and Rietveld refinements were performed with FullProf.[11] High pressure diamond anvil cells were used for all experiments. The culets of the diamond anvils were 300 μm in diameter. The ruby fluorescence technique[12] was used to measure pressure. High-pressure Raman measurements were made using a Coherent Innova 90 Plus argon ion laser to obtain the Raman spectra with the 514.5 nm laser line being used for excitation. The scattered light from the sample was focused into a Jobin-Yvon spectrograph equipped with a CCD detector.

First-principles electronic structure calculations were carried out using the plane-wave pseudopotential method within the framework of density functional theory with the software package VASP.[13] Projected augmented wave pseudopotentials[14] for Ca and H from the pseudopotential library were used. For Ca, $2p$ and $3s$ electrons were treated as valence. The Perdew-Wang 91 generalized gradient approximation exchange-correlation functional was employed. Monkhorst-Pack grids[15] of $12\times12\times12$ and $6\times12\times8$ were used for the electronic Brillouin zone integration in the hexagonal and orthorhombic structure, respectively. The cell shape and atomic positions were optimized at selected volumes and the corresponding pressures were computed from the stress tensor. Phonon calculations at the Brillouin zone center were carried out with the program ABINIT.[16] Trouiller-Martins-type pseudopotentials[17] employing an energy cutoff of 65 Hartree with the generalized gradient approximation of Perdew *et al.*[18] were employed.

RESULTS AND DISCUSSION

In run 1, x-ray diffraction patterns were collected after the loading of CaH_2 in the DAC. The pressure was initially at 16 GPa. The complicated powder x-ray diffraction pattern was found to be a mixture of the starting cotunnite structure with a minor unknown phase [Fig. 1(a)]. The intensity of the x-ray diffraction features attributed to the minority phase weakened when the pressure was released gradually from 16 GPa, which led to a full recovery of the pure cotunnite phase below 12 GPa. At 5 GPa the lattice parameters for the orthorhombic unit cell were $a=5.68(4)$, $b=3.51(2)$, and $c=6.66(2)$ Å. The sample was then recompressed from 5 GPa. Again, the diffraction patterns indicated the existence of a mixed phase at 15 GPa, but above 20 GPa the pattern became very simple, indicating the complete transformation to a higher symmetry phase. The diffraction pattern at 25 GPa was indexed to a hexagonal unit cell with $a=3.54(1)$ and $c=4.58(1)$ Å. The hexagonal cell can also be expressed as an equivalent orthorhombic cell with $a=4.58(1)$, $b=3.54(1)$, and $c=6.13(2)$ Å. The experimental equation of state shown in Fig. 2 indicates a first-order transition with a volume change of about 8% across the transition.

Significantly higher quality powder x-ray diffraction patterns [Fig. 1(b)] were subsequently measured on the HXMA beamline at CLS. In run 2, the initial pressure following loading of the sample in the DAC was below 1 GPa. The x-ray diffraction images could thus be recorded progressively as a function of increasing pressure. The x-ray diffraction pattern obtained at 5.2 GPa showed only the Bragg reflections from the ambient cotunnite structure giving unit cell parameters $a=5.760(9)$, $b=3.502(8)$, and $c=6.68(1)$ Å. In-

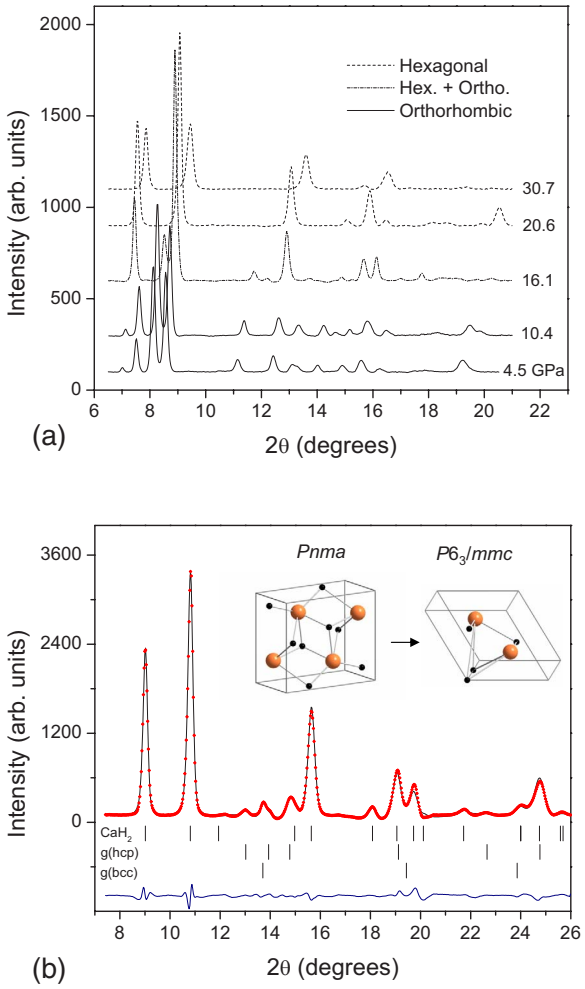

FIG. 1. (Color online) (a) (Top panel) X-ray diffraction pattern from run 1. Note that the initial pressure was 16 GPa in which the sample was already a mixture of the low pressure *Pnma* phase and high pressure $P6_3/mmc$ phase. The sample pressure was then decreased to 5 GPa and subsequently increased to finally reach 30 GPa. Background has been subtracted from all patterns and offsets have been introduced for clarity. (b) (Bottom panel) X-ray diffraction pattern (symbols) recorded at 22.9 GPa in run 2 and Rietveld fit (solid line) considering a mixture of three phases, namely, high-density CaH_2 ($P6_3/mmc$), hexagonal stainless steel gasket T301 ($P6_3/mmc$), and cubic stainless steel gasket T301 (Im-$3m$). For the CaH_2 phase, Ca atomic positions as fixed by symmetry and full site occupancies are assumed. Preferred orientation for the high-pressure hydride and the stainless steel gasket, both hexagonal phases, has been taken into account. The R factors for the Rietveld fit (FullProf) are $R_{exp}=7.8\%$, $R_{wp}=10.3\%$, and $R_{wp}/R_{exp}=1.3$. The bottom trace shows the difference between the Rietveld fit and the experimental data. The inset illustrates the low- and high-density structure models for CaH_2.

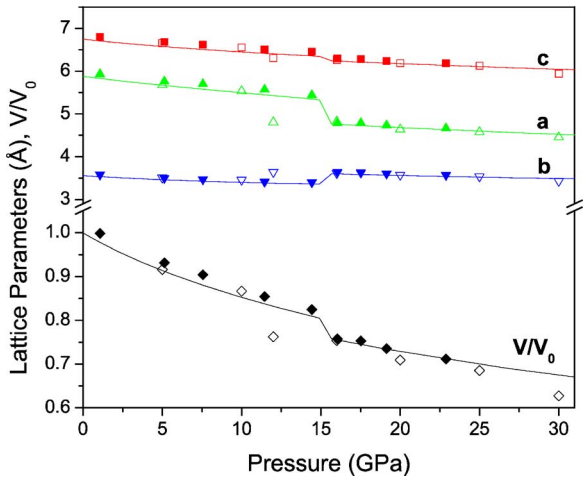

FIG. 2. (Color online) Room temperature pressure dependence of lattice parameters and relative unit cell volume of the orthorhombic *Pnma* and hexagonal $P6_3/mmc$ (in the orthorhombic setting) phases of CaH_2. Open and solid symbols distinguish results obtained in run 1 and run 2, respectively. Data points below 16 GPa were recorded with decreasing pressures in run 1. Solid lines represent theoretical calculations.

creasing pressure showed a phase transition at 14–16 GPa. Once again, the x-ray diffraction pattern of the high pressure phase can be indexed to a hexagonal unit cell ($P6_3/mmc$) with atoms at Wyckoff positions 2*c* (Ca), 2*d* (H), and 2*a* (H). At 22.9 GPa the equivalent orthorhombic cell parameters are $a=4.667(1)$, $b=3.571(3)$, and $c=6.185(6)$ Å. The x-ray diffraction pattern for the $P6_3/mmc$ phase observed at 22.9 GPa and the corresponding Rietveld fit are shown in Fig. 1(b). The Rietveld refinement was carried out with Ca^{+2} located at symmetry positions 2*c* (1/3, 2/3, 1/4) and full site occupancy and by taking into account preferred orientation, as was observed in the x-ray diffraction images of hexagonal CaH_2. X-ray scattering from hydrogen atoms was neglected. The small mismatch between the observed and model patterns [Fig. 1(b)] and x-ray diffraction arising for the gasket material can be explained most likely by preferred orientation not fully corrected and by less-than-optimal x-ray beam collimation. Owing to the better quality sample, improved x-ray diffraction resolution and the lack of overlapping patterns near the phase transition pressure, a more precise equation of state was obtained (Fig. 2). Results of run 2 confirmed the previous observation that a first-order structural phase transition occurs in CaH_2 and is found complete at 16 GPa.

High pressure Raman spectra for CaH_2 are reported in Fig. 3. In run 1, at 16.1 GPa, the Raman spectrum in the region 150–1000 cm^{-1} shows four bands centered at 180, 239, 290, and 840 cm^{-1} and a weak feature at 214 cm^{-1}. The four band Raman spectrum is in good agreement with a reported spectrum recorded under ambient condition.[6] Upon the release of pressure, the weak feature disappears below 12 GPa. This observation closely follows the variation of the diffraction patterns in run 1. Therefore, this weak band is almost certainly associated with the high pressure hexagonal phase which was mixed with the cotunnite phase from

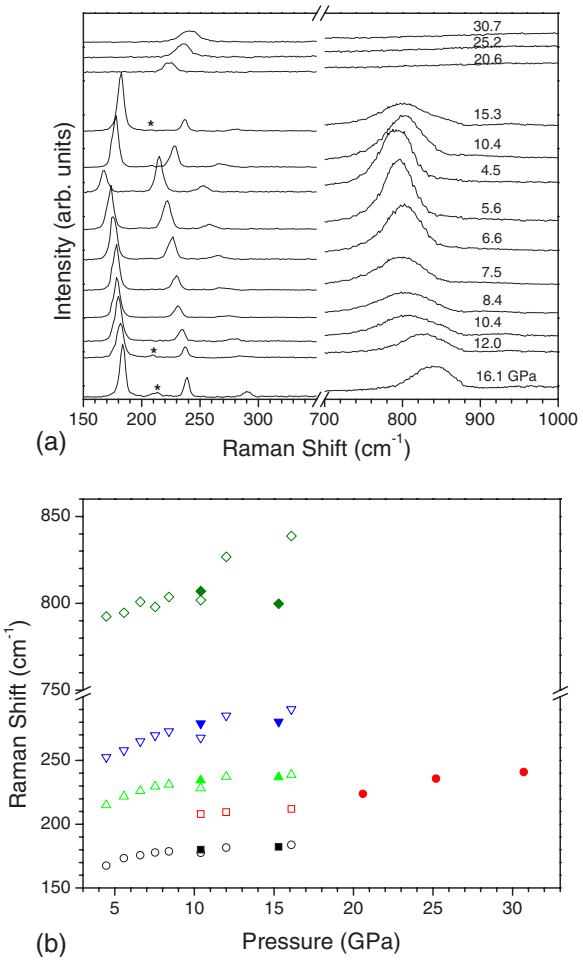

FIG. 3. (Color online) Raman data for run 1. (a) (Top panel) Raman spectra as a function of pressure, following the sequence of pressure changes from bottom to top. The asterisk indicates the Raman line due to the high-pressure phase in the case of phase mixtures. (b) (Bottom panel) Pressure dependence of the Raman shifts for decreasing pressures (open symbols) and increasing pressures (solid symbols).

12 to 16 GPa. When the CaH_2 sample is recompressed from 4.5 GPa, the four band Raman spectrum of the cotunnite structure is maintained until 15.3 GPa, upon which the small band at 200 cm^{-1} reemerges indicating the onset of the structural phase transition. At 20 GPa, the initial cotunnite spectral features vanished and a very simple one band Raman spectrum was observed up to 30.7 GPa, the highest pressure reached in run 1. The simplicity of the Raman spectrum again confirms that the high pressure phase indeed possesses a space group symmetry higher than the lower pressure orthorhombic *Pnma* phase. The variation of Raman band frequencies with pressure is shown in Fig. 3(b).

All experimental evidence unambiguously indicates that a first-order structural transformation occurs around 16 GPa in CaH_2. Analysis of the x-ray diffraction data suggests the high pressure phase has a hexagonal unit cell, which can also be represented by an orthorhombic unit cell. To characterize the structure of the high pressure phase and the mechanism of the transformation, first-principles electronic structure calculations were performed. The starting point of the calculation

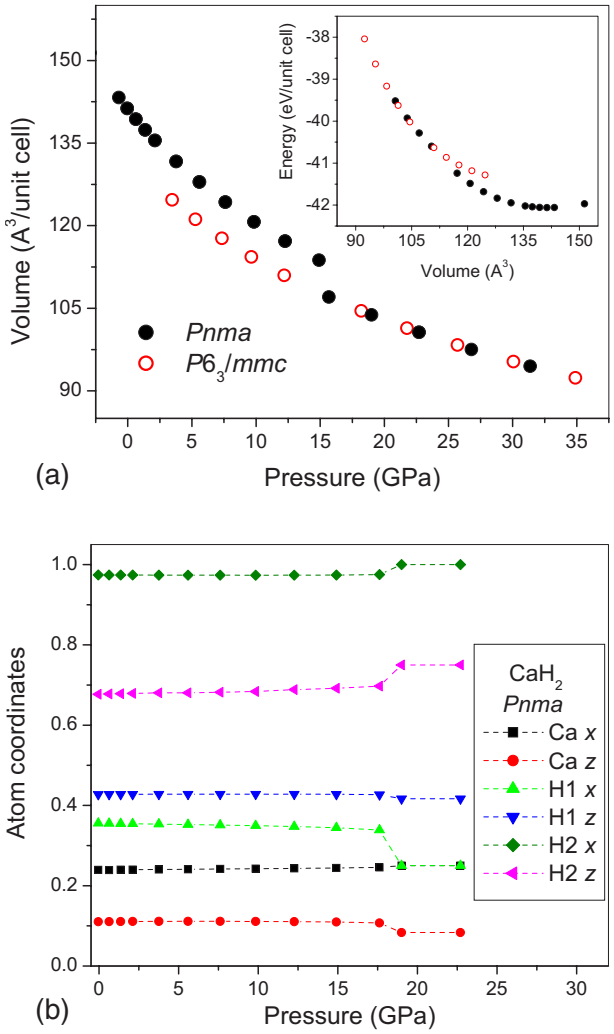

FIG. 4. (Color online) (a) (Top panel) Unit cell volume calculated as a function of pressure. The data points (open symbols) for the $P6_3/mmc$ are those for the equivalent orthorhombic setting. The inset illustrates the change of total energy for both phases. (b) (Bottom panel) Atomic coordinates calculated as a function of pressure.

was the ambient *Pnma* structure. Geometry optimization at 0 GPa gave a unit cell $a=5.881$, $b=3.559$, and $c=6.751$ Å and the following atomic positions: Ca ($x=0.2394$, $z=0.1104$), H_1 ($x=0.3556$, $z=0.4276$), and H_2 ($x=0.9742$, $z=0.6770$). These values compare favorably with the experimental neutron structure of CaD_2 (Ref. 8) of $a=5.925(1)$, $b=3.581(1)$, and $c=6.776(1)$ Å and Ca [$x=0.2378(13)$, $z=0.1071(8)$], D_1 [$x=0.3573(6)$, $z=0.4269(7)$], and D_2 [$x=0.9739(6)$, $z=0.6766(5)$]. Variation of the total energy and the volume of the *Pnma* phase of CaH_2 with pressure are shown in Fig. 4(a). These curves show a normal volume-pressure and energy-volume dependence until the pressure reaches 15 GPa. At this pressure the curves deviated and followed a different trend to higher pressures. The abrupt change in the energy is due to a structural phase transition. In the *Pnma* space group the Ca atoms and two unique H atoms occupy the Wyckoff 4*c* positions. The change in the internal atomic coordinates with pressure is shown in Fig. 4(b). At pressures below 17 GPa there are no significant changes in the atomic positions. However around 17 GPa, sudden shifts of the H_1 x coordinate and H_2 z coordinate to the special positions $\frac{1}{4}$ and $\frac{3}{4}$, respectively, were observed. Simultaneously the Ca position shifts to $(\frac{1}{4},\frac{1}{4},0)$. Analysis of the atomic positions revealed that the *Pnma* structure has transformed to hexagonal $P6_3/mmc$ with both the Ca and H located in special positions: $2c$ (Ca), $2d$ (H_1), and $2a$ (H_2). First-principles calculations in the higher symmetry $P6_3/mmc$ space group led to almost identical energies and unit cell volumes with the *Pnma* structure at pressures above 19 GPa [Fig. 4(b)]. Significantly, the calculated unit cell parameters in the orthorhombic representation are almost in quantitative agreement with the experimental observation as illustrated in Fig. 2. The discontinuities in the unit cell parameters observed at 16 GPa are clearly reproduced by the calculations. Since all the atoms are in symmetry sites, a Rietveld fit was carried out with preferred orientation of CaH_2 crystallites as the main correction, as shown in Fig. 1(b). The calculated diffraction patterns are in good agreement with experiment. In the high pressure hexagonal structure, the Ca atom is surrounded by three nearest neighbor H atoms and six second nearest neighbor H atoms. At 23 GPa, the calculated closest Ca [Fig. 1(b), inset] and H separations are 2.045, 2.315, and 2.350 Å. Each H atom is surrounded by five Ca atoms in a trigonal-pentagonal environment.

The theoretical high pressure CaH_2 structure is also consistent with spectral changes observed in the Raman spectra. It is expected the number of vibrational modes be reduced from a low- to high-symmetry structure. A factor group analysis on the $P6_3/mmc$ structure shows that only one Raman active band is expected in the 150–1000 cm^{-1} region. This prediction is verified by experiment as only one Raman peak is observed at pressure higher than 16 GPa. In fact, the calculated frequency for this band of 211 cm^{-1} at 19 GPa corresponds very well to the Raman band observed at 225 cm^{-1} at 20.6 GPa.

CONCLUSIONS

The crystalline structure of CaH_2 has been studied under high pressure up to 30 GPa. A structural phase transition from the ambient cotunnite *Pnma* structure to a hexagonal $P6_3/mmc$ structure has been unambiguously identified around 16 GPa from x-ray diffraction and Raman experiments and first-principles electronic calculations. The hexagonal phase is structurally identical to the $InNi_2$ structure ($P6_3$) predicted for high pressure MgH_2, however it has not been observed at pressures up to 57 GPa.[6] In contrast, in CaH_2, the phase transition occurs at substantially lower pressure. The present results suggest that the hexagonal structure should be achievable in MgH_2 at higher pressure. The hexagonal structure, however, remains an insulator and much higher pressure is needed to achieve metallization. Therefore, group II hydrides may not be convenient candidates for the exploration of superconductivity property at low pressure.

Note added in proof. We have been made aware of a previous high pressure x-ray study on CaH_2 (Ref. 19). The x-ray

diffraction, spectroscopic, and theoretical results presented here are in agreement with the x-ray diffraction results of Kinoshita *et al.*

ACKNOWLEDGMENTS

J.S.T. and S.D. acknowledge the financial support of NSERC. J.S.T. also wishes to thank the CFI and the Canada Research Chair Program for support. Raman and preliminary x-ray measurements were performed at the U2A and X17C beamlines at the NSLS of BNL (DOE Contract No. DE-AC02-98CH10886). The U2A and X17C beamlines are supported by COMPRES, the Consortium for Materials Properties Research in Earth Sciences under NSF Cooperative Agreement Grant No. EAR01-35554, and the U.S. Department of Energy (DOE) (CDAC Contract No. DE-FC03-03N00144). Additional x-ray experiments were performed at the Canadian Light Source, which is supported by NSERC, NRC, CIHR, and the University of Saskatchewan.

[1] A. W. MaClaine, U.S. Department of Energy, Office of Energy Efficiency and Renewable Energy, FY 2003, Progress Report of Hydrogen Fuel Cell and Technologies, Progress Report, 2003 (unpublished).
[2] V. C. Y. Kong, D. W. Kirk, F. R. Foulkes, and J. T. Hinatsu, Int. J. Hydrogen Energy **28**, 205 (2003).
[3] Y. Fukai and N. Okuma, Phys. Rev. Lett. **73**, 1640 (1994).
[4] P. Vajeeston, P. Ravindran, A. Kjekshus, and H. Fjellvåg, Phys. Rev. Lett. **89**, 175506 (2002).
[5] N. W. Ashcroft, Phys. Rev. Lett. **92**, 187002 (2004).
[6] T. Moriwaki, Y. Akahama, H. Kawamura, S. Nakano, and K. Takemura, J. Phys. Soc. Jpn. **75**, 074603 (2006); P. Vajeeston, P. Ravindran, B. C. Hauback, H. Fjellvåg, A. Kjekshus, S. Furuseth, and M. Hanfland, Phys. Rev. B **73**, 224102 (2006).
[7] E. Zintl and A. Harder, Z. Elektrochem. Angew. Phys. Chem. **41**, 33 (1935).
[8] A. F. Anderson, A. J. Maeland, and D. Slotfeldt-Ellingsen, J. Solid State Chem. **20**, 93 (1977).
[9] A. P. Hammersley, S. O. Svensonn, M. Hanfland, A. N. Fitch, and D. Häusermann, High Press. Res. **14**, 235 (1996); FIT2D, European Synchrotron Radiation Facility, 1998.
[10] S. Desgreniers and K. Lagarec, J. Appl. Crystallogr. **27**, 432 (1994); J. Appl. Crystallogr. **31**, 109 (1998).
[11] J. Rodrigues-Carvajal, Physica B **192**, 55 (1993); FullProf, version 3.70.
[12] H. K. Mao, J. Xu, and P. M. Bell, J. Geophys. Res., [Solid Earth Planets] **91B**, 4673 (1986).
[13] G. Kresse and J. Furthmüller, Comput. Mater. Sci. **6**, 15 (1996); Phys. Rev. B **54**, 11169 (1996).
[14] D. Vanderbilt, Phys. Rev. B **41**, 7892 (1990).
[15] H. J. Monkhorst and J. D. Pack, Phys. Rev. B **13**, 5188 (1976).
[16] X. Gonze, Phys. Rev. B **55**, 10337 (1997); X. Gonze and C. Lee, *ibid.* **55**, 10355 (1997); X. Gonze *et al.*, Comput. Mater. Sci. **25**, 478 (2002).
[17] N. Troullier and J. L. Martins, Phys. Rev. B **43**, 1993 (1991).
[18] J. P. Perdew, K. Burke, and M. Ernzerhof, Phys. Rev. Lett. **77**, 3865 (1996).
[19] K. Kinoshita *et al.*, *Proc 20th AIRAPT Conference*, (2005).